

Supporting Information: High temporal and bathymetric resolution of nautiloid death assemblages in stratigraphically-condensed oozes (New Caledonia)

Adam Tomašových, Ján Schlögl, Darrell S. Kaufman, Natália Hudáčková

1. Methods - age calibration

2. Differences between the prismatic and nacreous layer

3. Shell preservation

4. Last appearances of foraminifers

1. Methods - age calibration

Material. Twenty-one dead shells of *Nautilus macromphalus* were collected with beam trawls and dredges at eleven sites (off Lifou Island, off Isle of Pines, and off Great Southern Reef) around the New Caledonia archipelago in 1985 and 1987 (Fig. S1, Table S1). They are deposited at the Université de Bourgogne in Dijon. In addition, five specimens described by Mapes et al. (2010a) were obtained from the American Natural History. They were sampled at Lansdowne Bank (located between New Caledonia and the Chesterfield Islands) and the Antigonía Seamount in 2003 and 2005.

Amino-acid racemization (AAR). Small portions of shell were chipped from the outer chamber whorls of 26 specimens. These fragments were split into external prismatic and middle nacreous layers that were analyzed separately for the extent of amino acid racemization (AAR) at Northern Arizona University using reverse-

phase high-pressure liquid chromatography (RP-HPLC) and the procedures of Kaufman and Manley (1998) (with the exception of specimen CP 42/1 where the nacreous layers was not preserved). Specimens were leached 10% by weight with a dilute solution of HCl. To recover the total hydrolysable amino acid population, the shells were dissolved in 7M HCl and the resulting solutions were hydrolysed at 110°C for 22 hours to release amino acids from their peptide chains. This process can induce some racemization, especially of amino acids that racemize at higher rates (Kaufman and Manley 1998).

To minimize the effects of intra-layer variation in amino acid compositions and D/L values (e.g., Goodfriend et al. 1997; Torres et al. 2013) and to minimize ontogenetic effects (Goodfriend and Weidman 2001), we sampled only the whorl chamber or ontogenetically oldest portions of specimens. Concentrations and D/L values of eight amino acids were measured, including aspartic acid (Asp), glutamic acid (Glu), serine (Ser), alanine (Ala), valine (Val), phenylalanine (Phe), isoleucine (Ile), and leucine (Leu). Asp and Glu acid were used in age calibrations because these amino acids are analytically the most precisely resolved, with highest reproducibility (Kaufman and Manley 1998). The six other amino acids were used in screening and comparative analyses of two shell layers. We use three screening criteria described by Kosnik and Kaufman (2008) to detect aberrant specimens. To detect outliers, specimens were tested for strength of correlation between (1) Ser concentrations that can indicate contamination (standardized by the concentration of Glu), (2) total concentrations of Asp and Glu, and (3) Asp D/L^e and Glu D/L, where e is an exponent that linearizes the trend. All of the data showed strong internal consistency and were retained, except one (the prismatic layer of specimen DW43, which was flagged as an outlier by the third criterion, Fig. S2).

Radiocarbon ages. Eight specimens were dated with ^{14}C at the AMS facility at the Poznan Radiocarbon Laboratory in 2014 (Table S2). To avoid contamination, 30% of the outer shell mass was removed prior to AMS analysis in an ultrasonic bath and in 0.5M HCl, then treated in 15% H_2O_2 again (for 10 min in a ultrasonic bath). The remaining carbonate was dissolved with concentrated H_3PO_4 in a vacuum line. ^{14}C was measured with a "Compact Carbon AMS" (Goslar et al. 2004) by comparing intensities of ionic beams of ^{14}C , ^{13}C and ^{12}C measured for individual specimens and for standards (modern standard: "Oxalic Acid II" and standard of ^{14}C -free carbon: "background"). Conventional ^{14}C ages were calculated using correction for isotopic fractionation (Stuiver and Polach 1977), on the basis of ratio $^{13}\text{C}/^{12}\text{C}$ measured in the AMS spectrometer simultaneously with the ratio $^{14}\text{C}/^{12}\text{C}$. Specimen CP45/4 returned a post-bomb age (107.74% modern carbon) and one specimen had ^{14}C activity indistinguishable from background, implying an age of >50,000 years.

Calendar ages. Radiocarbon ages of the remaining six specimens were converted to calendar years using Calib6.0 (Stuiver and Reimer 1993) and the Marine13 data (Reimer et al. 2013). A regional marine reservoir correction (ΔR) was determined to be 26 years (standard deviation = 23 years) on the basis of the ^{14}C age of five marine samples of bivalves and corals from New Caledonia and Vanuatu in the Marine Reservoir Correction Database (calib.qub.ac.uk/marine). The reported calendar ^{14}C age is the median of the age probability function, with the two sigma age range (Table S2).

AMS-AAR calibration. Six ^{14}C -dated specimens were used to calibrate the rate of AAR. In addition, one specimen collected in 2003 and dated as 19 years old (thus 30 years old when analyzed for AAR in 2014) by ^{210}Pb (Mapes et al. (2010a) was also used

in AMS-AAR calibration. We calibrated the rate of AAR using the Bayesian model fitting procedures according to Allen et al. (2013). Asp and Glu D/L values were fit separately for two layers (nacreous and prismatic) using four mathematical functions to model the relation between age and D/L values, and two uncertainty models (lognormal and gamma) using R language (R Development Core Team 2013). The four mathematical functions include time-dependent rate kinetics (TDK), constrained power-law kinetics (CPK), simple power-law kinetics (SPK), with and without fitting a non-zero initial D/L. We use Bayesian model averaging to infer final ages, using all models that are not larger than two BIC units relative to the model with the smallest BIC. Final age corresponds to median age based on posterior distribution of ages predicted by calibration models (that differ in kinetics, uncertainty structure, and amino acids) weighted by evidence supporting each model.

The combination of two shell layers, two amino acids, two uncertainty models, two types of intercepts, and four functions gives 64 different age models. The models with Bayesian information criterion (BIC) values less than two units relative to the minimum BIC value have a strong basis for successful calibration (Kass and Raftery 1995), and those with BIC values less than six units have good basis for calibration, with APK1 model showing the best support for Asp (nacreous) and Glu (prismatic), and TDK1 and TDK0 for Glu (nacreous) and Asp (prismatic) (Fig. 1, Fig. S3, Table S3). The shells were collected between 1985 and 2005. The reported calibrated ages are thus adjusted relative to the year of collection from the seafloor. They were rounded to the nearest decade (Table S4).

Asp D/L values in the prismatic and nacreous layer show similar relations with postmortem age but with a constant offset, with higher D/L values in the prismatic layer (Fig. 1). Glu D/L values are similar between the two layers (Fig. 1). Although D/L values of live-collected specimens are not available, the shell with the youngest ages (28 years at time of AAR measurement) shows a much higher D/L value in the prismatic layer than in the nacreous layer (by a factor of 1.7).

Calibrations with different functions behave rather similarly and show similar BIC values (Table S3). Models using gamma uncertainty have tendency to overestimate the ages of younger shells (see also Allen et al. 2013), the lognormal uncertainty does not overestimate ages of shells with less than 1,000 years, in contrast to the gamma uncertainty. The residuals of younger shells are also more randomly distributed around zero in models with lognormal uncertainty.

2. Differences between the prismatic and nacreous layer

The external prismatic and middle nacreous layers significantly differ in the amino acid composition and racemization ratios, with higher proportions and higher D/L values of the Asp in the prismatic layer (Fig. S4). Proteins of the prismatic layer are dominated by Asp (median = ~60%), with other amino acids contributing with ~10%. Concentrations of all amino acids significantly decline with age in the nacreous layer (Fig. S4).

The correlations between individual D/L values of eight amino acids and between amino acid concentrations within nacreous layer are higher than within the prismatic layer. The correlations between ^{14}C and eight amino acids are higher in the nacreous layer, similar to rank correlations between all D/L values of all amino acids, and rank correla-

tions between their concentrations (Fig. S4). With the exception of one specimen (1150 years old), total amino acid concentrations are higher in the nacreous layer. The external prismatic layer seems to be more affected by bacterial contamination (Fig. S5), and thus probably represents a diagenetically less-closed system than the middle nacreous layer.

3. Shell preservation

The phragmocone walls of each specimen were assigned to three incompleteness categories (almost complete phragmocones, partly preserved phragmocones, and specimens with umbilical relicts). Boxplots show that incomplete relicts are older than specimens with complete phragmocones (Fig. S6). X-ray diffraction analyses of a powder extracted from external coatings and microboring infills from the specimen CP272 revealed the dominance of goethite and clay minerals (chlorite, kaolinite). Muscovite, quartz and albite were also detected. The chemical composition of clay matrix among detritic grains in external coatings and microborings (5 measurement spots) was analysed (specimen CP232) with wave-dispersion X-ray microanalysis, using a JXA-8530F electron microprobe. Operating conditions were 1 μm spot resolution, 15 kV accelerating voltage and 15-20 nA sample current. The relative standard deviation is less than $\pm 5\%$. These analyses show weight percents of SiO_2 (28.6-31.2%), Al_2O_3 (16-17.8%), $\text{FeO}_{\text{total}}$ (18.5-27.8%), K_2O (0.94-1.87%), MgO (2.46-4.26), and CaO (0.94-1.63%). The coatings thus correspond to goethite-clay aggregates and can represent incipient stages of glauconitization.

4. Last appearances of foraminifers

Carchariostomoides dentaliniformis - 0.67 Myr (Hayward et al. 2012)

Globigerinoides obliqua extrema - 1.8 Myr (Hayward et al. 2015), 2.5 Myr (BouDagher-Fadel 2012)

pink *Globigerinoides rubra* - 0.126 Myr (Thompson et al. 1979)

Globigerinoides fistulosus - 1.88 Myr (Gradstein et al. 2004), latest Pleistocene (BouDagher-Fadel 2012)

Globigerinoides trilobus - 0.78 Myr (Hayward et al. 2015)

Neogloboquadrina acostaensis - 1.585 Myr (Gradstein et al. 2004)

Pulleniatina praecursor - 1.8 Myr (Kennet and Srinivasan 1983), middle Pleistocene (BouDagher-Fadel 2012)

Siphonodosaria lepidula - 0.57 Myr (Hayward et al. 2012)

Sphaeroidinellopsis paenedehiscens - 1.926 Myr (Kennet and Srinivasan 1983)

Strictocostella advena - 0.8 Myr (Hayward et al. 2012)

Strictocostella scharbergana - 0.53 Myr (Hayward et al. 2012)

Strictocostella at genus level - 0.5 Myr (Hayward et al. 2012)

References

Allen, A.P., Kosnik, M.A., and Kaufman, D.S., 2013, Characterizing the dynamics of amino acid racemization using time-dependent reaction kinetics: A Bayesian approach to fitting age-calibration models. *Quaternary Geochronology*, **18**, 63-77.

BouDagher-Fadel, M.K., 2012, Biostratigraphic and geological significance of planktonic Foraminifera. *Developments in Palaeontology and Stratigraphy*, **22**, 1-301.

Goodfriend, G.A., Flessa, K.W., and Hare, P.H., 1997, Variation in amino acid epimerization rates and amino acid composition among shell layers in the bivalve *Chione* from the Gulf of California. *Geochimica et Cosmochimica Acta*, **61**, 1487–1493.

Goodfriend G.A., and Weidman, C.R., 2001, Ontogenetic trends in aspartic acid racemization and amino acid composition within modern and fossil shells of the bivalve *Arctica*. *Geochimica et Cosmochimica Acta*, **65**, 1921–1932.

Goslar T., Czernik J., and Goslar, E., 2004, Low-energy ¹⁴C AMS in Poznań Radiocarbon Laboratory, Poland. *Nuclear Instruments and Methods B*, **223-224**, 5-11.

Gradstein F., Ogg J., and Smith, A., 2004, A Geological Time Scale 2004. Cambridge University Press.

Hayward, B.W., Kawagata, S., Sabaa, A.T., Grenfell, H.R., Van Kerckhoven, L., Johnson, K., and Thomas, E., 2012, The last global extinction (mid-Pleistocene) of deep-sea benthic foraminifera (Chrysalogoniidae, Ellipsoidinidae, Glandulonodosariidae, Plectofrondiculariidae, Pleurostomellidae, Stilostomellidae), their late Cretaceous-Cenozoic history and taxonomy. *Cushman Foundation for Foraminiferal Research, Special Publication*, **43**, 1-408.

Hayward, B.W., Cedhagen, T., Kaminski, M., Gross, O., 2015, World Foraminifera Database: Accessed at <http://www.marinespecies.org/foraminifera>.

Kass, R.E., and Raftery, A.E., 1995, Bayes Factors. *Journal of the American Statistical Association*, **90**, 773–795.

- Kaufman, D.S., and Manley, W.F., 1998, A new procedure for determining DL amino acid ratios in fossils using reverse phase liquid chromatography. *Quaternary Science Reviews*, **17**, 987–1000.
- Kennett, J. and Srinivasan, M.S., 1983, Neogene Planktonic Foraminifera - A Phylogenetic Atlas: Hutchinson Ross.
- Mapes, R.H., Landman, N.H., Cochran, K., Goiran, C., De Forges, B.R. and Renfro, A., 2010a, Early taphonomy and significance of naturally submerged *Nautilus* shells from the New Caledonia region. *Palaios*, **25**, 597-610.
- Reimer, P., Bard, E., Bayliss, A., Beck, J., Blackwell, P., Bronk Ramsey, C., Buck, C., Cheng, H., Edwards, R., Friedrich, M., Grootes, P., Guilderson, T., Haflidason, H., Hajdas, I., Hatté, C., Heaton, T., Hoffmann, D., Hogg, A., Hughen, K., Kaiser, K., Kromer, B., Manning, S., Niu, M., Reimer, R., Richards, D., Scott, E., Southon, J., Staff, R., Turney, C., and van der Plicht, J., 2013, IntCal13 and Marine13 radiocarbon age calibration curves 0–50,000 years cal BP. *Radiocarbon*, **55**, 1869-1887.
- Stuiver, M., and Polach, H.A., 1977, Discussion: reporting of ^{14}C data. *Radiocarbon*, **19**, 355–63.
- Thompson, P.R., Bé, A.W.H., Duplessy, J.-C., and Shackleton, N.J., 1979, Disappearance of pink-pigmented *Globigerinoides ruber* at 120,000 yr BP in the Indian and Pacific oceans. *Nature*, **280**, 554-558.
- Torres, T., Ortiz, J.E., and Arribas, I., 2013, Variations in racemization/epimerization ratios and amino acid content of *Glycymeris* shells in raised marine deposits in the Mediterranean. *Quaternary Geochronology*, **16**, 35-49.

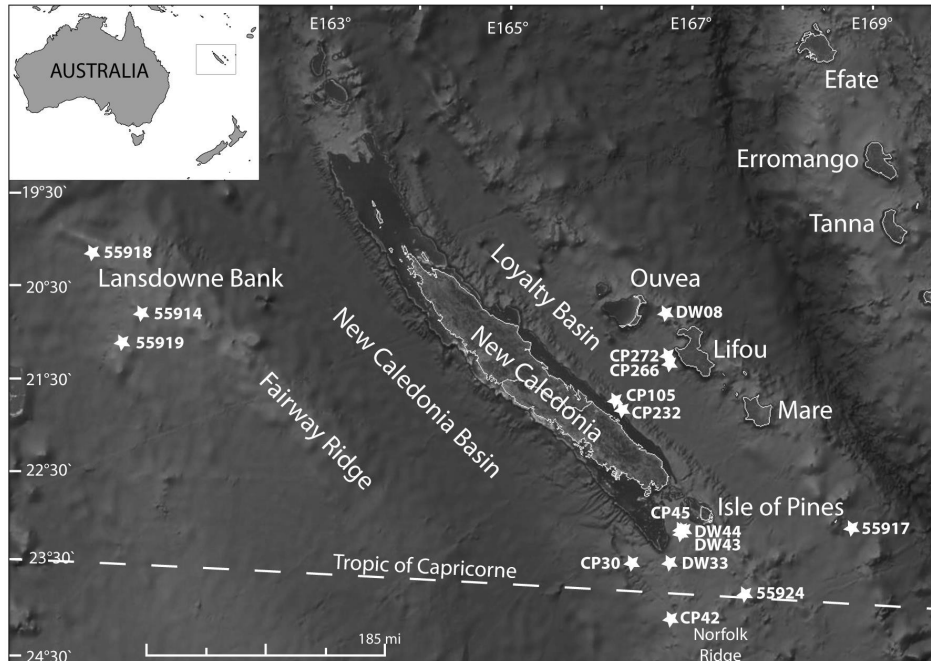


Figure S1 - Location of stations where dead shells of *Nautilus macromphalus* were collected for this study. Google Earth (Version 7.1.2.2041) [Software]. Mountain View, CA: Google Inc. (2014).

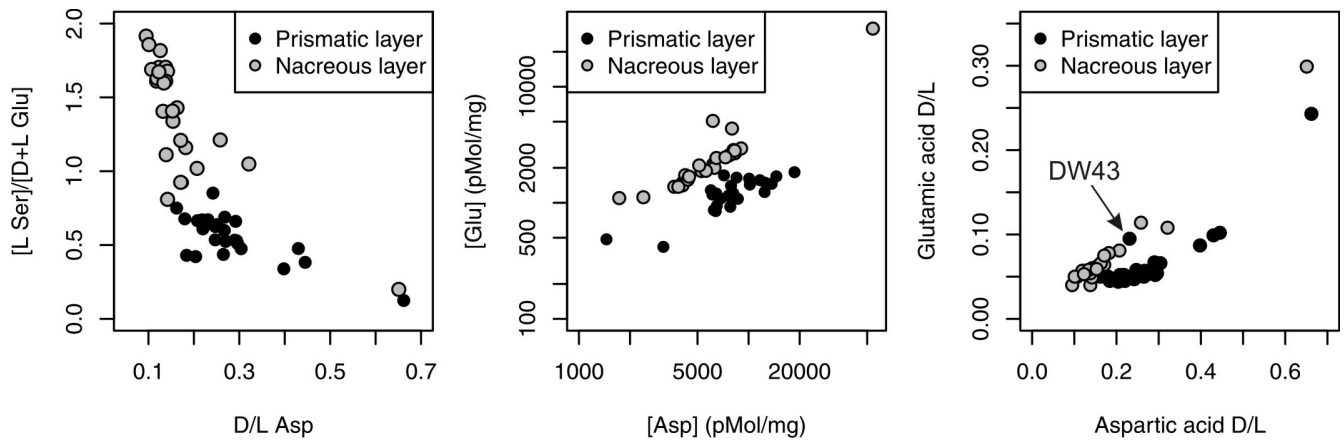


Figure S2 - Data screening. A. L-serine concentrations ($[L-Ser]$) relative to glutamic acid concentrations ($[D+L Glu]$) against aspartic acid (Asp) D/L. B. Concentrations of Asp relative to Glu. C. Asp D/L relative to Glu D/L, showing that Asp is more racemized in the prismatic layer. The prismatic layer of DW43 was detected as an outlier.

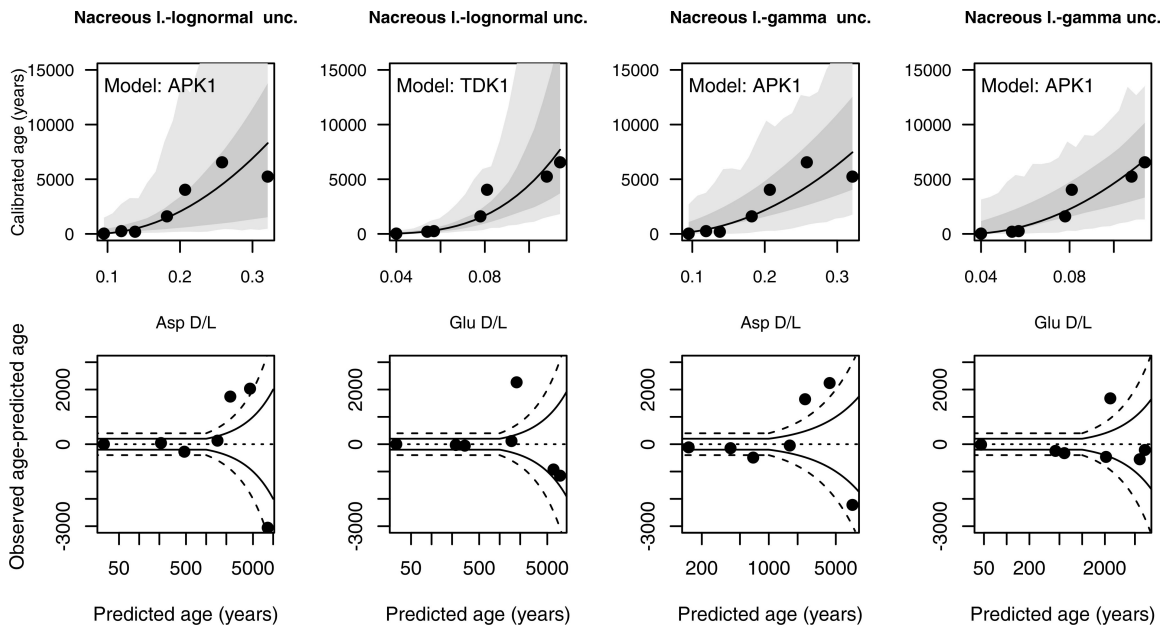


Figure S3 - Top row: Relation between postmortem age (determined by ^{14}C and ^{210}Pb) and D/L values of two amino acids for the prismatic and nacreous layers, best-fit by TDK1 and CPK0 models, respectively, representing the best fits on the basis of BIC, and assuming log-normal and gamma distributions for the residuals. Light grey envelopes correspond to 95% prediction intervals for the age of a given specimen, dark grey correspond to 95% confidence intervals for median age. Bottom row: Age differences between calendar and Asp- and Glu-inferred ages. The solid lines indicate age differences of 200 years or 20%, and the dashed lines indicate age differences of 400 yr or 40%.

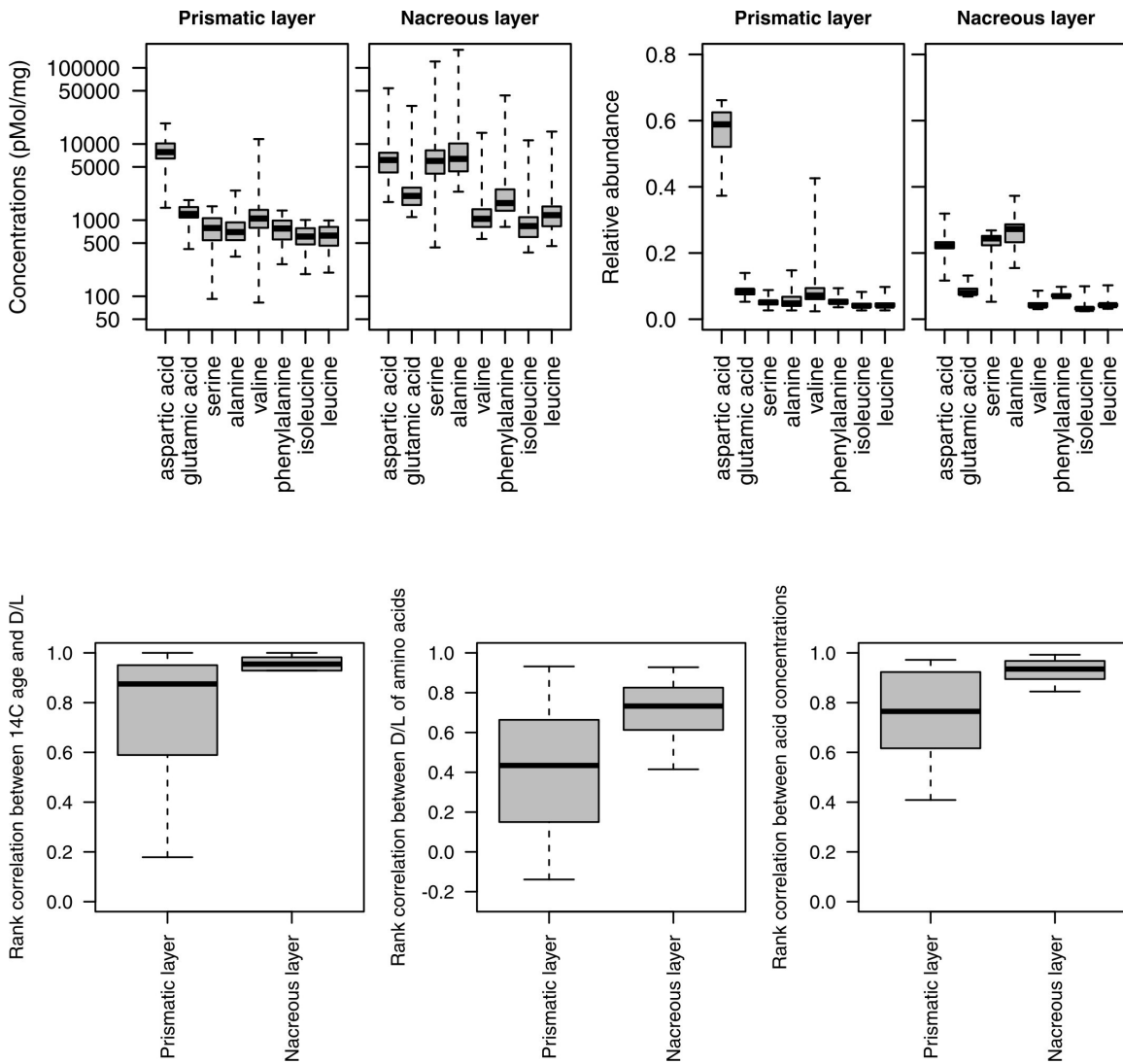


Figure S4 – Top row: Box-and-whisker plots showing the concentrations and relative abundances of eight amino acids in the prismatic and nacreous layers. Nacreous layers tend to have higher concentrations of seven acids other than the aspartic acid, which dominates the prismatic layer. The nacreous layer contains higher relative abundance of serine and alanine. Bottom row: Correlations between (A) D/L value and shell ^{14}C age, (B) concentrations of eight amino acids, and (C) D/L values of eight amino acids. All correlations are higher, and therefore the internal consistency of results is greater in the nacreous than in the prismatic layer, implying more closed system during sea-floor diagenesis in the nacreous layer.

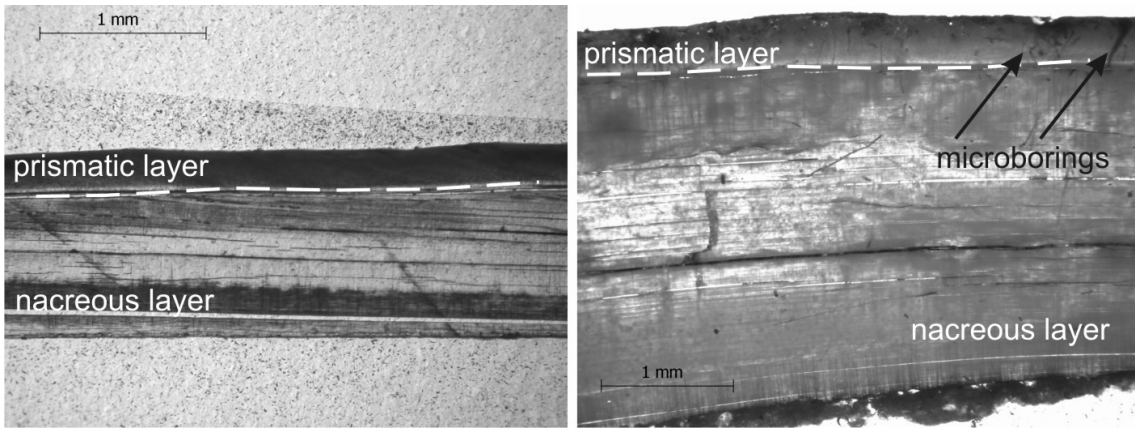


Figure S5 - Cross-section photomicrographs of the external prismatic and the middle nacreous layer showing a higher degree of microbioerosion in the external prismatic layer (upper part) than in the thicker nacreous layer. The left figure corresponds to the pristine specimen CP272.

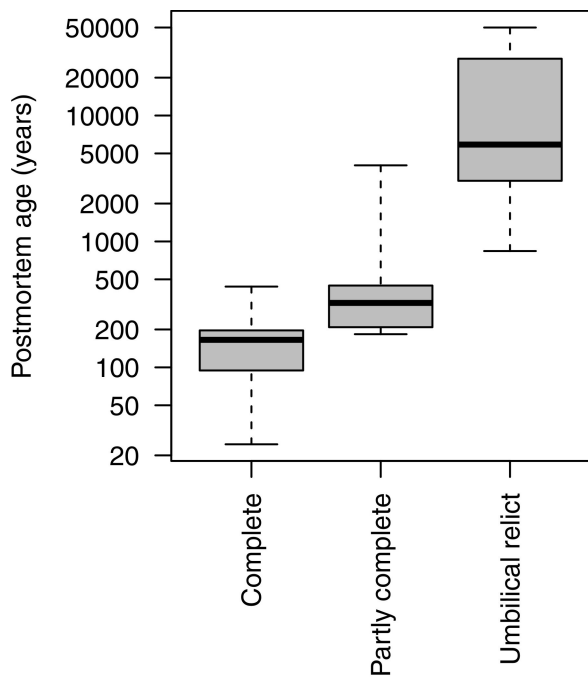


Figure S6 - Incomplete relicts are significantly older than specimens with complete phragmocones. The thick black horizontal lines represent medians, the box boundaries represent the 25th and 75th percentiles, and whiskers capture the minima and maxima of postmortem ages.

Table S1 - Geographic coordinates and water depths of 26 specimens of *Nautilus macromphalus*, with information on the presence of extinct foraminifers (with times of their last appearance). See text for references on times of last appearance of foraminifers.

Specimen number	Sampling year	Latitude	Longitude	Water depth (m)	Sampling gear	Extinct foraminifers
55914	2005	-20.79883	161.0035	418	dredge	no sediment preserved
55917	2003	-22.69683	169.16167	313	dredge	no sediment preserved
55918	2005	-20.09767	160.37183	532	dredge	no sediment preserved
55919	2005	-21.08467	160.79033	672	dredge	no sediment preserved
55924	2003	-23.38117	168.01433	383	dredge	no sediment preserved
CP105	1985	-21.51183	166.362	330-335	beam trawl	no sediment preserved
CP232	1987	-21.5635	166.451167	760-790	beam trawl	<i>pink Globigerinoides rubra</i> (0.126 Myr)
CP266	1987	21.08083	166.95233	1990-2100	beam trawl	<i>pink Globigerinoides rubra</i> (0.126 Myr), <i>Sphaeroidinellopsis paenedehiscens</i> (1.9 Myr), <i>Globigerinoides trilobus</i> (0.78 Myr), <i>Pulleniatina</i>
CP272	1987	-21.00067	166.949	1615-1710	beam trawl	<i>praecursor</i> (1.8 Myr)
CP30/2	1985	-23.1608	166.6808	1140	beam trawl	no sediment preserved
CP30/3	1985	-23.1608	166.6808	1140	beam trawl	no sediment preserved
CP30/5	1985	-23.1608	166.6808	1140	beam trawl	no sediment preserved
CP30	1985	-23.1608	166.6808	1140	beam trawl	no sediment preserved
CP42/1	1985	-23.7523	167.202	380	beam trawl	no sediment preserved
CP45/1	1985	-22.789	167.2467	430	beam trawl	<i>Globigerinoides fistulosus</i> (1.88 Myr), <i>Strictocostella scharbergana</i> (0.53 Myr), <i>Strictocostella scharbergana</i> (0.53 Myr), <i>Strictocostella advena</i> (0.8 Myr),
CP45/2	1985	-22.789	167.2467	430	beam trawl	<i>Globigerinoides trilobus</i> (0.78 Myr)
CP45/3	1985	-22.789	167.2467	430	beam trawl	<i>Pulleniatina praecursor</i> (1.8 Myr)
CP45/4	1985	-22.789	167.2467	430	beam trawl	no sediment preserved <i>Globigerinoides obliqua extrema</i> (1.8 Myr), <i>Globigerinoides fistulosus</i> (1.88 Myr),
DW08	1985	-20.5725	166.8983	435	dredge	<i>Globigerinoides trilobus</i> (0.78 Myr)
DW33/1	1985	-23.1618	167.1712	675-680	dredge	<i>Globigerinoides trilobus</i> (0.78 myr) <i>Carchariostomoides dentaliniformis</i> (0.67 Myr), <i>Siphonodosaria lepidula</i> (0.57 Myr),
DW33/2	1985	-23.1618	167.1712	675-680	dredge	<i>Globigerinoides obliqua extrema</i> (1.8 Myr) <i>Globigerinoides fistulosus</i> (1.88 Myr), <i>Neogloboquadrina acostaensis</i> (1.6 Myr), <i>Globigerinoides obliqua extrema</i> (1.8 Myr), <i>Globigerinoides trilobus</i> (0.78 Myr), <i>Sphaeroidinellopsis paenedehiscens</i> (1.9 Myr),
DW43	1985	-22.7702	167.2417	400	dredge	<i>Strictocostella</i> sp. (0.5 Myr)
DW44/1	1985	-22.7883	167.2383	440-450	dredge	<i>Strictocostella scharbergana</i> (0.53 Myr) <i>Sphaeroidinellopsis paenedehiscens</i> (1.9 Myr), <i>Globigerinoides fistulosus</i> (1.88 Myr), <i>Globigerinoides obliqua extrema</i> (1.8 Myr),
DW44/2	1985	-22.7883	167.2383	440-450	dredge	<i>Globigerinoides trilobus</i> (0.78 Myr) <i>Sphaeroidinellopsis paenedehiscens</i> (1.9 Myr),
DW44/3	1985	-22.7883	167.2383	440-450	dredge	<i>Strictocostella</i> sp. (0.5 Myr)
CP30/4	1985	-23.1608	166.6808	1140	beam trawl	extant species only

Table S2 - Radiocarbon (and ^{210}Pb for the specimen 55924) ages used to calibrate the rate of amino acid racemization. Specimen ages refer to 2014 when amino acid composition was completed. For example, the specimen 55924 was sampled in 2003 and Mapes et al. (2010) estimated its age as 19 years. Its amino acid composition was measured in 2014, and postmortem age used in AAR-AMS calibration is thus 30 years.

Poznan laboratory number	Specimen code	Water depth (m)	^{14}C age (yr BP)	Age error (yr)	Maximum calibrated age (before 2014)	Minimum calibrated age (before 2014)	Calibrated age (year before 2014)
NA	55924	383	NA	NA	47	15	30
Poz-59170	DW33/2	675-680	4895	42	5356	5098	5240
Poz-62246	CP45/2	430	535	38	310	103	198
Poz-62247	CP232	760-790	585	38	346	133	254
Poz-65873	DW33/1	675-680	6090	46	6685	6442	6549
Poz-65874	CP30/5	1140	2010	42	1729	1478	1606
Poz-65871	CP30/2	1140	4000	42	4160	3903	4036
Poz-62244	CP30/4	1140	>50,000	NA	NA	NA	Old
Poz-62245	CP45/4	430	107.74±0.27 pMC	NA	NA	NA	Modern

Table S3 – Calibration statistics for the rate of amino acid racemization (AAR) based on paired AAR and radiometric analyses of *Nautilus macromphalus* and two models of uncertainty. Models with BIC values less than 2 units relative to the model with minimum BIC are shown. Explanations: k = number of parameters; APK = apparent parabolic kinetics; CPK = constrained power-law kinetics; SPK = simple power-law kinetics; TDK = time-dependent reaction kinetics; 0 = the initial D/L value is fixed at zero; 1 = the initial D/L value is estimated from data.

Acid	Model	Log(a)	Log(b)	c	Log(R0)	Log(d)	k	deviance	BIC	delta.bic
Nacreous layer: lognormal uncertainty										
glutamic	TDK1	16.476	1.117	0.445	-3.617	-2.382	4	98.89	106.68	0.000
glutamic	APK1	13.713	NA	1.136	-3.356	-1.662	3	101.96	107.80	1.124
glutamic	SPK0	20.305	1.636	NA	NA	-1.806	3	102.29	108.13	1.455
glutamic	TDK0	20.689	1.664	NA	NA	-1.756	3	102.31	108.15	1.472
glutamic	SPK1	19.519	1.564	1.237	-3.333	-2.098	4	100.39	108.17	1.492
Prismatic layer: lognormal uncertainty										
aspartic	TDK0	12.526	1.640	NA	NA	-1.199	3	105.62	111.46	0.000
aspartic	SPK0	13.142	1.704	NA	NA	-1.285	3	105.88	111.72	0.259
aspartic	CPK0	0.912	2.140	NA	NA	-1.248	3	105.90	111.73	0.271
aspartic	CPK1	2.251	1.923	0.958	-2.005	-1.205	4	105.64	113.42	1.960
aspartic	TDK1	12.578	1.648	-7.795	-35.190	-1.350	4	105.64	113.43	1.965
Nacreous layer: gamma uncertainty										
glutamic	APK1	13.839	NA	0.893	-3.425	5.329	3	103.73	109.56	0.000
glutamic	SPK0	16.635	1.274	NA	NA	5.739	3	104.81	110.65	1.087
glutamic	TDK0	16.681	1.281	NA	NA	5.704	3	104.82	110.66	1.098
Prismatic layer: gamma uncertainty										
glutamic	APK1	14.395	NA	0.981	-3.174	4.864	3	100.71	106.54	0.000
glutamic	TDK1	13.787	0.569	1.262	-3.105	4.715	4	100.94	108.73	2.181

Table S4 - Postmortem ages used in the construction of age-frequency distribution (relative to time since collection of shells on the sea-floor) with the corresponding D/L values for the external spherulitic-prismatic layer and the middle nacreous layer. The ages were rounded to the nearest decade. Postmortem ages are based on the ^{14}C and ^{210}Pb ages of seven shells in Table S2, the AAR ages of the additional 17 shells are based on the calibration of the nacreous layer. The AAR age of the specimen CP42/1 is based on the prismatic layer because its nacreous layer was poorly preserved.

Specimen ID	Depth (m)	Postmortem age (y)	Prismatic Asp D/L	Prismatic Glu D/L	Nacreous Asp D/L	Nacreous Glu D/L
55914	418	285.9	0.247	0.058	0.126	0.057
55917	313	232	0.251	0.052	0.123	0.055
55918	532	240.5	0.208	0.052	0.118	0.055
55919	672	140.8	0.18	0.05	0.107	0.05
55924	383	19	0.162	0.05	0.095	0.04
CP105	332.5	245	0.204	0.044	0.132	0.056
CP232	775	227	0.265	0.05	0.119	0.057
CP266	2045	13.8	0.175	0.051	0.138	0.04
CP272	1662.5	165.9	0.247	0.051	0.139	0.052
CP30/2	1140	4007	0.398	0.087	0.207	0.081
CP30/3	1140	499.5	0.29	0.067	0.171	0.064
CP30/5	1140	1577	0.304	0.066	0.182	0.078
CP30	1140	105.9	0.268	0.052	0.142	0.049
CP42/1	380	97.2	0.22	0.045	NA	NA
CP45/1	430	358.4	0.292	0.052	0.142	0.06
CP45/2	430	169	0.294	0.059	0.138	0.054
CP45/3	430	415.6	0.27	0.052	0.154	0.062
CP45/4	430	122.3	0.184	0.045	0.101	0.05
DW08	435	280.2	0.218	0.052	0.134	0.058
DW33/1	680	6520	0.445	0.102	0.258	0.114
DW33/2	680	5211	0.43	0.099	0.321	0.108
DW43	400	580.8	0.231	0.095	0.163	0.066
DW44/1	445	324.2	0.267	0.057	0.153	0.059
DW44/2	445	172.5	0.242	0.047	0.123	0.053
DW44/3	445	1119.3	0.296	0.054	0.171	0.075
CP30/4	1140	50000	0.662	0.243	0.651	0.299

Table S5 - Parameters of three models (one-phase exponential, Weibull, and two-phase exponential model) fitted to two age-frequency distributions, with AIC and BIC values. For one-phase and two-phase exponential models, half-lives of nautiloid loss from the mixed layer correspond to $\log(2)/\lambda$. The disintegration rate parameters of the two-phase exponential model (λ_1 and λ_2) imply that the initial half-life of nautiloid shells is 211 years (total assemblage), 195 years (epibathyal) or 268 years (mesobathyal) whereas the half-life of degraded relicts can be much longer - 9902 years (total assemblage), 3013 years (epibathyal), or ~17,000 years (mesobathyal, but the sample size is small).

	Total assemblage	Epibathyal assemblage	Mesobathyal assemblage
N (sample size)	26	18	8
One-phase lambda	0.00036	0.00109	0.00014
Weibull r	0.36	0.02	72.35
Weibull k	0.26	0.43	0.16
Two-phase lambda 1	0.00328	0.00356	0.00259
Two-phase lambda 2	0.00007	0.00023	0.00004
Two-phase tau	0.000016	0.000041	0.000017
One-phase AICc	467.1	283.9	160.5
Weibull AICc	419.4	276.8	144.4
Two-phase AICc	415.6	276.1	153.4
One-phase BIC	468.2	284.5	159.9
Weibull BIC	421.4	277.8	142.1
Two-phase BIC	418.3	277	147.6

Table S6 - Foraminifers found in ooze sediments within whorls of 14 shells.

Species name	Author	CP30/4	DW33/1	CP45/2	CP45/1	CP45/3	CP266	DW44/1	CP272	DW44/2	DW8	DW43	CP232	DW44/3	DW33/2
<i>Alveolophragmium zealandicum</i>	Vella, 1957	0	0	0	0	1	0	0	0	0	0	0	0	0	0
<i>Ammobaculites agglutinans</i>	(d'Orbigny, 1846)	0	0	0	0	0	0	0	0	0	0	0	0	1	0
<i>Ammobaculites villosus</i>	Saidova, 1975	0	0	0	0	0	0	0	0	1	0	0	0	0	0
<i>Ammodiscus gullmarensis</i>	Höglund, 1948	0	0	0	0	1	0	0	0	0	0	0	0	0	0
<i>Amphicoryna hirsuta</i>	(d'Orbigny, 1826)	0	0	0	0	0	0	0	0	0	0	0	0	1	0
<i>Amphicoryna scalaris</i>	(Batsch, 1791)	0	0	1	0	1	0	0	0	0	0	0	0	0	0
<i>Amphicoryna separans</i>	(Brady, 1884)	0	1	0	0	0	0	1	0	1	0	0	0	0	0
<i>Amphistegina</i> sp.	d'Orbigny, 1826	0	1	0	0	0	0	0	0	0	0	0	0	0	0
<i>Armorella sphaerica</i>	Heron-Allen & Earland, 1932	0	0	0	0	1	0	0	0	0	0	0	0	0	0
<i>Astacolus crepidulus</i>	(Fichtel & Moll, 1798)	0	0	0	0	0	0	0	0	0	0	1	0	1	0
<i>Asterigerinata mamilla</i>	(Williamson, 1858)	0	0	0	0	1	0	0	0	0	0	0	0	0	0
<i>Bolivina</i> ex gr. <i>dilatata</i>	Reuss, 1850	0	0	0	0	0	0	0	1	0	0	0	0	0	0
<i>Bolivina robusta</i>	Brady, 1881	0	0	0	0	0	0	0	0	0	0	0	0	1	0
<i>Bolivina</i> sp.	d'Orbigny, 1839	0	0	0	0	0	0	0	1	1	0	1	0	0	0
<i>Bolivina spathulata</i>	(Williamson, 1858)	0	0	0	0	1	0	0	0	0	0	1	0	0	0
<i>Bolivina subreticulata</i>	Parr, 1932	0	0	0	0	0	0	0	0	0	0	0	1	0	0
<i>Bulimina striata</i>	d'Orbigny in Guérin-Méneville, 1843	0	0	0	0	0	0	0	0	0	0	0	0	1	0
<i>Calcarina hispida</i>	Brady, 1876	0	0	0	1	0	0	0	0	0	0	0	0	0	0
<i>Candeina nitida</i>	d'Orbigny, 1839	0	0	0	0	0	1	0	1	0	1	0	0	0	0
<i>Carchariostomoides dentaliniformis</i>	(Cushman & Jarvis, 1934) †	0	0	0	0	0	0	0	0	0	0	0	0	0	1
<i>Cassidulina carinata</i>	Silvestri, 1896	0	0	0	0	0	0	0	0	0	0	1	0	0	0
<i>Cassidulina globosa</i>	Hantken, 1865	0	0	0	0	0	0	0	0	0	0	1	0	0	0
<i>Cassidulina laevigata</i>	d'Orbigny, 1826	0	0	0	0	1	0	0	1	0	0	0	0	1	0
<i>Cassidulina</i> sp.	d'Orbigny, 1826	0	0	0	0	1	0	0	0	0	0	0	0	0	0
<i>Cibicides haidingeri</i>	(d'Orbigny, 1846)	0	0	0	0	1	0	0	0	0	0	1	0	0	0
<i>Cibicides refulgens</i>	de Montfort, 1808	0	0	1	1	0	1	0	0	1	0	0	0	1	0
<i>Cibicides wuellerstorfi</i>	(Schwager, 1866)	0	0	1	1	1	0	1	0	1	1	1	0	1	0
<i>Cibicoides subhaidingeri</i>	(Parr, 1950)	0	0	0	0	0	0	0	0	0	0	0	0	1	0
<i>Cymbaloporetta grandis</i>	(Cushman, 1934)	0	0	0	0	0	0	1	0	0	0	1	0	0	0
<i>Discanomalina coronata</i>	(Parker & Jones, 1865)	0	0	0	1	0	0	1	0	1	0	0	0	0	0
<i>Discorbina planorbis</i>	(d'Orbigny, 1846)	0	0	0	0	0	0	1	0	0	0	0	0	0	0
<i>Dorothyia bradyana</i>	Cushman, 1936	0	0	0	0	0	0	0	0	1	0	0	0	0	0
<i>Dorothyia</i> cf. <i>scabra</i>	(Brady, 1884)	0	0	0	0	0	0	0	0	0	0	1	0	0	0
<i>Dorothyia</i> sp.	Plummer, 1931	0	0	0	1	1	0	2	0	1	0	0	0	0	0
<i>Duquepsammia bulbosa</i>	(Cushman, 1911)	0	0	0	1	0	0	1	0	0	0	0	0	1	0
<i>Eggerella bradyi</i>	(Cushman, 1911)	0	0	1	0	0	0	0	0	0	0	0	0	0	0
<i>Elongobula</i> sp.	Finlay, 1939	0	0	0	0	0	0	1	0	0	0	0	0	0	0
<i>Fissurina laevigata</i>	Reuss, 1850	1	0	0	0	0	0	0	0	0	0	0	0	0	0
<i>Fissurina</i> sp.	Reuss, 1850	0	0	0	1	0	0	0	0	0	0	0	0	0	0
<i>Gaudryina robusta</i>	Cushman, 1913	0	0	0	2	0	0	1	0	0	0	1	0	0	0
<i>Glandulina</i> sp.	d'Orbigny, 1839	0	0	0	0	0	0	0	0	0	0	1	0	0	0
<i>Globigerina</i> aff. <i>nepenthes</i>	Todd, 1957 †	1	0	0	0	0	0	0	0	0	0	0	0	0	0
<i>Globigerina bulloides</i>	d'Orbigny, 1826	1	0	0	0	1	0	1	0	1	0	1	0	1	0
<i>Globigerina falconensis</i>	Blow, 1959	0	0	0	1	1	0	1	1	1	0	1	0	0	0
<i>Globigerinella obesa</i>	(Bolli, 1957)	1	0	0	0	0	0	0	0	0	0	1	0	0	0
<i>Globigerinella siphonifera</i>	(d'Orbigny, 1839)	0	0	1	1	1	1	1	1	0	1	1	0	0	0
<i>Globigerinita glutinata</i>	(Egger, 1893)	1	0	0	0	0	0	0	0	0	0	0	0	1	0
<i>Giobigenoides conglobata</i>	(Brady, 1879)	0	1	0	1	1	1	0	1	1	1	0	0	1	0

Table S7 - Concentrations of amino acids in the prismatic and nacreous layers

Specimen ID	D/L Asp	D/L Glu	D/L Ser	D/L Ala	D/L Val	D/L Phe	D/L Ile	D/L Leu	L Asp	D Asp	L Glu	D Glu	L Ser	D Ser
Prismatic layer														
55914	0.247	0.058	0.119	0.090	0.049	0.042	0.044	0.054	12063	2983	1677	97	1110	132
55917	0.251	0.052	0.136	0.138	0.030	0.040	0.045	0.059	13457	3375	1855	97	1246	170
55918	0.208	0.052	0.078	0.094	0.047	0.038	0.024	0.055	14192	2952	1623	85	1136	89
55919	0.180	0.050	0.073	0.104	0.046	0.041	0.027	0.056	15235	2742	1824	92	1298	95
55924	0.162	0.050	0.044	0.103	0.043	0.039	0.022	0.060	19100	3088	2079	103	1637	72
CP105	0.204	0.044	0.094	0.061	0.034	0.039	0.158	0.061	9345.9	1906.6	1633.4	71.1	718.6	67.5
CP232	0.265	0.050	0.140	0.101	0.015	0.043	0.115	0.073	9592	2538	1691	85	775	108
CP266	0.175	0.051	0.043	0.070	0.015	0.050	0.028	0.061	7953	1396	1903	97	1846	79
CP272	0.247	0.051	0.134	0.095	0.028	0.047	0.119	0.070	7781	1921	1223	62	688	95
CP30/2	0.398	0.087	0.326	0.118	0.098	0.080	0.023	0.085	6807.8	2709.2	1214.2	106.2	447.5	146.1
CP30/3	0.290	0.067	0.171	0.082	0.043	0.063	0.062	0.061	3826	1111	614	41	349	60
CP30/5	0.304	0.066	0.218	0.100	0.020	0.068	0.042	0.076	7695	2337	1364	90	691	150
CP30	0.268	0.052	0.143	0.091	0.018	0.044	0.134	0.069	9354	2503	2008	105	1455	208
CP42/1	0.220	0.045	0.110	0.082	0.027	0.055	0.026	0.045	10512	2308	1702	76	1084	119
CP45/1	0.292	0.052	0.117	0.083	0.049	0.043	0.149	0.069	8581	2502	1675	86	1163	136
CP45/2	0.294	0.059	0.169	0.089	0.027	0.053	0.062	0.072	12334	3631	2415	144	1353	229
CP45/3	0.270	0.052	0.115	0.099	0.022	0.049	0.110	0.061	11176.7	3012.3	2007.9	104.2	1108.6	127.6
CP45/4	0.184	0.045	0.091	0.084	0.081	0.054	0.040	0.062	10097.4	1858.7	1354.2	61.6	609	55.7
DW08	0.218	0.052	0.067	0.068	0.026	0.043	0.032	0.047	10939.7	2386.1	1586.4	81.9	1118.6	75
DW33/1	0.445	0.102	0.307	0.135	0.041	0.110	0.105	0.131	6984.7	3105.6	1710	174.2	721	221.1
DW33/2	0.430	0.099	0.310	0.131	0.036	0.120	0.093	0.120	6326.3	2722.5	1582	156.3	828.1	257
DW43	0.231	0.095	0.114	0.077	0.016	0.050	0.063	0.059	9260.5	2141.2	2503.5	237.5	1839.9	210.5
DW44/1	0.267	0.057	0.132	0.071	0.039	0.059	0.079	0.085	14281.6	3808.7	2297.1	131.3	1453.1	192.5
DW44/2	0.242	0.047	0.084	0.046	0.021	0.059	0.055	0.076	10460.3	2535.4	2407.7	112.3	2146.4	179.3
DW44/3	0.296	0.054	0.159	0.088	0.026	0.055	0.097	0.061	11690.5	3465.9	2029.1	110.5	1094.6	173.8
CP30/4	0.662	0.243	0.531	0.542	0.135	0.457	0.178	0.528	11149	7383	4971	1208	769	408
Nacreous layer														
55914	0.126	0.057	0.083	0.039	0.017	0.039	0.020	0.061	8851	1116	3034	172	5826	486
55917	0.123	0.055	0.096	0.037	0.018	0.039	0.023	0.042	6476	795	2388	131	4290	413
55918	0.118	0.055	0.060	0.041	0.027	0.040	0.026	0.058	8791	1040	3253	179	5527	330
55919	0.107	0.050	0.054	0.033	0.019	0.041	0.029	0.091	9026	961	3092	156	5486	296
55924	0.095	0.040	0.020	0.028	0.013	0.029	0.017	0.043	35507	3383	21924	873	43657	869
CP105	0.132	0.056	0.081	0.039	0.016	0.043	0.038	0.040	5387	712	2105	119	3126	254
CP232	0.119	0.057	0.072	0.040	0.017	0.047	0.026	0.052	8764	1043	3120	177	5372	387
CP266	0.138	0.040	0.048	0.031	0.014	0.034	0.012	0.046	12687	1756	7587	303	13444	640
CP272	0.139	0.052	0.159	0.039	0.015	0.050	0.023	0.040	3253	404	1624	78	1892	276
CP30/2	0.207	0.081	0.261	0.078	0.030	0.107	0.030	0.096	8240	1704	2924	237	3222	840
CP30/3	0.171	0.064	0.201	0.064	0.019	0.084	0.012	0.073	5505	942	2095	134	2061	415
CP30/5	0.182	0.078	0.180	0.062	0.024	0.081	0.039	0.075	5476	996	2452	192	3067	554
CP30	0.142	0.049	0.102	0.115	0.017	0.051	0.013	0.055	7980	1133	7157	353	6079	622
CP42/1	NA	NA	NA	NA	NA	NA	NA	NA	NA	NA	NA	NA	NA	NA
CP45/1	0.142	0.060	0.098	0.041	0.019	0.059	0.022	0.057	6105	865	2372	142	4217	412
CP45/2	0.138	0.054	0.129	0.038	0.017	0.047	0.024	0.048	10752	1487	3878	210	6581	846
CP45/3	0.154	0.062	0.124	0.047	0.021	0.053	0.014	0.056	4960.9	765.7	2032.1	126	2887.8	356.7
CP45/4	0.101	0.050	0.036	0.033	0.019	0.038	0.014	0.033	12320.2	1239.3	4389.4	220.2	8562.1	308.7
DW08	0.134	0.058	0.072	0.041	0.018	0.047	0.018	0.049	7053.5	943	2690.3	156.3	4546.5	326
DW33/1	0.258	0.114	0.329	0.097	0.050	0.131	0.046	0.133	7317.7	1884.6	2780.7	317	3753.5	1234.9
DW33/2	0.321	0.108	0.406	0.120	0.053	0.166	0.063	0.130	4407.8	1413.7	1872.7	201.4	2175.4	882.4
DW43	0.163	0.066	0.171	0.044	0.021	0.055	0.031	0.049	5814	948.1	2389.9	156.6	3640	620.8
DW44/1	0.153	0.059	0.108	0.046	0.029	0.056	0.045	0.070	8709.4	1331.9	3571.9	211.3	5324.7	575.9
DW44/2	0.123	0.053	0.074	0.037	0.017	0.041	0.035	0.047	10239.7	1255	3685.2	194.2	6488.6	479.1
DW44/3	0.171	0.075	0.145	0.053	0.022	0.054	0.071	0.069	58702.5	10066.8	26239.5	1974.1	34112.3	4961.2
CP30/4	0.651	0.299	0.761	0.564	0.203	0.639	0.241	0.623	1653	1077	1335	399	346	264

Specimen	Gly	L Ala	L hArg	D Ala	L Val	D Val	L Phe	L Ile	D Phe	L Leu	D alle	D Leu
Prismatic layer												
55914	7372	1075	239	96	772	38	1180	829	50	924	36	50
55917	7570	644	231	89	996	29	1487	1026	60	1064	46	63
55918	7980	952	276	90	680	32	1142	870	44	814	21	45
55919	7908	915	263	95	854	39	1245	1081	51	980	29	55
55924	10805	1008	238	104	859	37	1458	1171	57	1033	26	62
CP105	5547.3	891.7	296	54.3	539.1	18.2	792.5	554.7	31.1	639.6	87.8	39.3
CP232	5177	780	314	78	604	9	889	696	38	691	80	51
CP266	4794	1259	312	88	1454	22	1117	1108	56	1185	31	72
CP272	4283	584	303	56	623	17	790	622	37	593	72	40
CP30/2	5130	587.6	305	69.2	475.9	46.7	666.3	499	53.1	539.8	11.6	46.1
CP30/3	2334	482	314	39	285	12	390	289	24	303	18	18
CP30/5	4943	727	309	73	654	13	803	711	54	664	30	50
CP30	4751	924	301	84	1274	23	1363	1172	59	989	157	68
CP42/1	5965	923	312	76	808	22	1224	805	67	894	21	41
CP45/1	5615	1375	324	114	759	37	1113	782	48	826	117	57
CP45/2	7146	1607	317	142	1342	37	1486	1273	79	1313	79	95
CP45/3	6077.1	977.1	350	96.8	885.7	19.3	1236.2	903.3	61.1	1038.3	99	63.3
CP45/4	6156	691.6	307	58	421	34.1	763.1	500.3	41.1	579	19.9	36
DW08	6314.7	867.5	308	58.8	718.2	18.4	1065.9	757.3	45.7	829.4	24.3	39
DW33/1	4860.9	1473.4	313	198	869.6	35.5	1021.6	806.4	112.2	851.7	84.9	111.5
DW33/2	3906.6	1209	296	159	912.5	32.4	1056.8	899.1	126.4	870	83.4	104.7
DW43	5648.6	3572.2	318	275	1703	27	1664.4	1347.1	82.8	1489.2	84.9	87.9
DW44/1	8106.3	1942.4	310	137	1236.4	48.6	1503.9	1125.6	88.4	1244.7	89	105.4
DW44/2	8685	3579.8	306	165	1026.3	22	1574.5	1015.9	93.4	1208.2	56.1	91.6
DW44/3	6588.8	993.3	298	87.2	1048.4	27.6	1388.2	983.1	75.8	1067.3	95.5	64.8
CP30/4	7962	3348	2551	1815	3530	476	2842	3096	1300	2822	551	1488
Nacreous layer												
55914	13688	13173	240	509	1602	28	2929	1287	115	1717	26	105
55917	9095	9163	235	335	1299	24	2173	1022	85	1334	24	56
55918	12217	11754	241	488	1804	50	3008	1375	121	1847	35	106
55919	11553	10898	221	363	1585	30	2849	1249	116	1674	37	152
55924	106896	120767	144	3436	9968	127	30392	7918	878	10048	135	432
CP105	6669	5142	298	200	1193	19	1734	861	74	1106	33	45
CP232	10385	11498	317	457	1621	28	2867	1291	134	1752	33	92
CP266	28399	38611	362	1201	3615	50	9400	2724	319	3473	34	159
CP272	3786	3489	305	114	927	13	1367	622	61	891	14	32
CP30/2	9329	7027	316	546	1401	42	2248	1026	240	1206	31	116
CP30/3	5468	3579	316	230	877	17	1273	587	107	672	7	49
CP30/5	6569	6034	306	372	1296	31	1892	995	154	1225	39	92
CP30	13772	8455	296	973	5173	89	4926	6000	253	5926	75	324
CP42/1	NA	NA	NA	NA	NA	NA	NA	NA	NA	NA	NA	NA
CP45/1	8858	9068	318	370	1180	23	1996	907	118	1250	20	72
CP45/2	16063	16417	319	618	1941	32	3599	1532	170	2109	37	100
CP45/3	6261	5056.1	314	240	1124.4	23.8	1565.1	797	83.7	1030.7	11.4	57.3
CP45/4	16696	17204.4	328	572	2237.3	43.1	4078.9	1754.3	154	2399.3	23.9	78.7
DW08	10624	9214.1	303	373	1417.1	25.3	2287.7	1060.5	106.4	1427.9	18.9	69.5
DW33/1	12377	11438.3	328	1114	1423.7	71.1	2432.8	1148.3	318.7	1520.2	53	202
DW33/2	6157.6	5896.2	302	709	947.6	50.1	1423.7	748.9	236.1	922.7	47.2	120.4
DW43	9228.8	7481.8	303	331	1235.6	26.2	2148.9	980.9	118.4	1281	30.8	62.4
DW44/1	9740	10914.8	311	502	2268.7	65.1	2934.6	1755.8	165.1	2178.1	78.6	153.1
DW44/2	12931	14082.2	315	522	2032.6	33.6	3444.4	1586.1	141.5	2126.5	56.3	99.1
DW44/3	64058	67491.4	2688	3561	16931.1	372	20417.7	12916.8	1099.8	15490.6	917.1	1065.5
CP30/4	2276	2461	316	1389	877	178	786	576	502	668	139	417

